Journal of Hazardous Materials 307 (2016) 253–262

Contents lists available at ScienceDirect

Journal of Hazardous Materials

journal homepage: www.elsevier.com/locate/jhazmat

Validating carbonation parameters of alkaline solid wastes via integrated thermal analyses: Principles and applications

Shu-Yuan Pan[a], E.-E. Chang[b], Hyunook Kim[c], Yi-Hung Chen[d], Pen-Chi Chiang[a,*]

[a] Graduate Institute of Environmental Engineering, National Taiwan University, Taipei 10673, Taiwan
[b] Department of Biochemistry, Taipei Medical University, Taipei 110, Taiwan
[c] Department of Environmental Engineering, University of Seoul, Seoul 130-743, South Korea
[d] Department of Chemical Engineering and Biotechnology, National Taipei University of Technology, Taipei 10608, Taiwan

HIGHLIGHTS

- Key carbonation parameters of wastes are determined by integrated thermal analyses.
- A modified TG-DTG interpretation is proposed, and validated by the DSC technique.
- The modified TG-DTG interpretation is further verified by DTA, TG-MS and TG-FTIR.
- Kinetics and thermodynamics of $CaCO_3$ decomposition in solid wastes are determined.
- Implication to maximum carbonation conversion of various solid wastes is described.

GRAPHICAL ABSTRACT

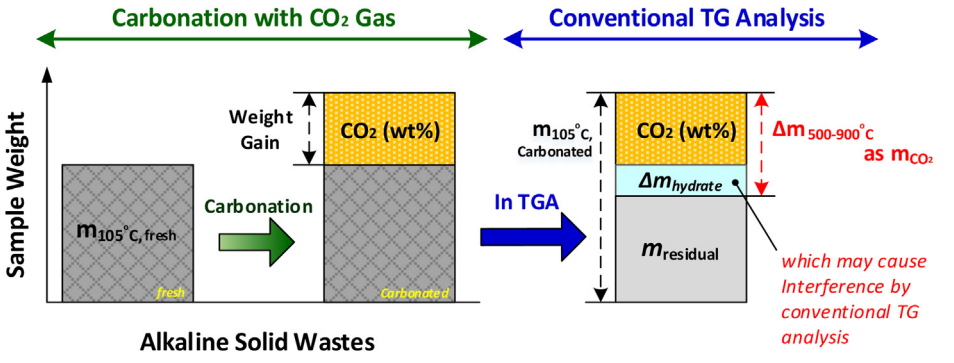

ARTICLE INFO

Article history:
Received 22 October 2015
Received in revised form
29 December 2015
Accepted 30 December 2015
Available online 4 January 2016

Keywords:
Stabilization
CO_2 fixation
Mineralization
Analytical
Kissinger equation

ABSTRACT

Accelerated carbonation of alkaline solid wastes is an attractive method for CO_2 capture and utilization. However, the evaluation criteria of $CaCO_3$ content in solid wastes and the way to interpret thermal analysis profiles were found to be quite different among the literature. In this investigation, an integrated thermal analyses for determining carbonation parameters in basic oxygen furnace slag (BOFS) were proposed based on thermogravimetric (TG), derivative thermogravimetric (DTG), and differential scanning calorimetry (DSC) analyses. A modified method of TG-DTG interpretation was proposed by considering the consecutive weight loss of sample with 200–900 °C because the decomposition of various hydrated compounds caused variances in estimates by using conventional methods of TG interpretation. Different quantities of reference $CaCO_3$ standards, carbonated BOFS samples and synthetic $CaCO_3$/BOFS mixtures were prepared for evaluating the data quality of the modified TG-DTG interpretation, in terms of precision and accuracy. The quantitative results of the modified TG-DTG method were also validated by DSC analysis. In addition, to confirm the TG-DTG results, the evolved gas analysis was performed by mass spectrometer and Fourier transform infrared spectroscopy for detection of the gaseous compounds released during heating. Furthermore, the decomposition kinetics and thermodynamics of $CaCO_3$ in BOFS was evaluated using Arrhenius equation and Kissinger

* Corresponding author. Fax: +886 2 23661642.
E-mail addresses: pcchiang@ntu.edu.tw, d00541004@ntu.edu.tw (P.-C. Chiang).

http://dx.doi.org/10.1016/j.jhazmat.2015.12.065
0304-3894/

equation. The proposed integrated thermal analyses for determining $CaCO_3$ content in alkaline wastes was precise and accurate, thereby enabling to effectively assess the CO_2 capture capacity of alkaline wastes for mineral carbonation.

1. Introduction

Recently, interest in the accelerated carbonation of alkaline solid wastes (e.g., steelmaking slags) has sharply escalated due to their potential to fix gaseous CO_2 from industry into solid precipitation (e.g., calcium carbonate), that could mitigate global climate change [1–4]. Moreover, the physico-chemical properties of solid wastes can be improved by carbonation, thereby increasing the potential for being used as construction materials such as supplementary cementitious materials and/or aggregates in civil engineering [5]. To evaluate and compare the performance of accelerated carbonation provided by various types of approach and process, thermo-analytical techniques, including thermogravimetric (TG) analysis, derivative thermogravimetric (DTG), differential thermal analysis (DTA), and differential scanning calorimetry (DSC) have commonly been utilized to quantify carbonation products such as calcium carbonate ($CaCO_3$) in solid wastes. Other analytical techniques, such as reference intensity ratio method [6] and Rietveld refinement [7] using X-ray diffraction, can also provide quantitative analysis on the carbonate products in solid wastes. Although X-ray techniques can provide precise and accurate information on the fraction of crystal phases, they are generally time-consumed in sample preparation and data processing.

TG analysis was considered as a rapid and accurate method for the determination of crystalline $CaCO_3$ content in highly pure samples [8]. However, in the case of cementitious materials such as concrete and cement [9], it was difficult to realize accurate quantitative profiles of $CaCO_3$ content using only TG data because (1) the way to interpret TG curves for $CaCO_3$ decomposition in a material was varied among researchers; and (2) the temperature ranges of thermal decomposition of $CaCO_3$ overlap the calcareous and hydrated components in these materials. Similar challenges were observed for carbonation of alkaline solid wastes such as basic oxygen furnace slag (BOFS) because their physico-chemical properties are similar to those of cementitious materials.

Two of the most commonly used methods for determining the weight loss of a certain material by interpreting TG curve were (1) delta-Y and (2) on-set methods, as shown in Fig. 1. The delta-Y method is to determine the difference of sample weight directly between two specific temperatures (e.g., T_1 and T_2 in Fig. 1), while the on-set method is to extend the straight line portions of the baseline and the linear portion of the upward/downward slope, mark their intersection, and determine the weight difference between these two intersections. It is noted that there is a significant difference in the determined weight loss for the same TG plot. In particular, in the case of BOFS, the dehydration of calcium silicate hydrates, calcium aluminate hydrates, and other minor hydrates was found to occur between 105 and 1000 °C, resulting in a continuous and steady weight loss [10]. Although it is especially pronounced at temperatures less than 500 °C, consideration must be given to weight loss due to dehydration of the above materials at 500–900 °C. Otherwise, the $CaCO_3$ contents in BOFS will be overestimated by the conventional delta-Y or on-set methods.

Table 1 summarizes the analytical conditions of TG and temperature ranges of the thermal decomposition of $Ca(OH)_2$, $MgCO_3$, and $CaCO_3$ contained in different solid wastes, such as steelmaking slags, coal combustion fly ash, cement kiln dust, and municipal solid wastes, in the literature. As noticed by Table 1, the evaluation criteria of carbonate products by TG analysis were quite different among the literature because of the wide variance in determining the temperature ranges of product decomposition. This is also largely due to the various ways to interpret TG curve, thereby resulting in different bases on performance evaluation of CO_2 capture capacity for carbonation. Thus, a validated method needs to be developed for accurately quantifying the $CaCO_3$ content in solid wastes.

In this investigation, a method determining carbonation parameters in alkaline solid wastes via integrated thermal analysis was developed and evaluated, as presented in Fig. 2. The integrated thermal analyses were performed based on TG, DTG and DSC analyses, in conjunction with a mass spectrometer (MS) and Fourier transform infrared spectroscopy (FTIR). A modified method of TG-DTG interpretation was proposed by considering the consecutive weight loss of sample with 200–900 °C due to the decomposition of various hydrated compounds. The objectives of this study were (1) to determine the $CaCO_3$ content in BOFS by modified interpretation using both TG and DTG curves, (2) to validate the data quality of the TG-DTG method via DSC technique; (3) to verify the TG-DTG results by the supporting evidence of qualitative observation, including DTA, TG-MS and TG-FTIR; and (4) to elucidate kinetic and thermodynamic behaviors of $CaCO_3$ decomposition in BOFS based on the Arrhenius equation, Kissinger equation, and transition state theory (see Appendix A).

2. Materials and methods

2.1. Materials

The fresh BOFS was provided by a steelmaking company (Kaohsiung, Taiwan). The as-received BOFS was carbonated with pure CO_2 gas via a rotating packed bed under mild conditions [2,5]. According to our previous report [5], the BOFS was rich in CaO (~48.2%), Fe_2O_3 (~26.0%) and SiO_2 (~8.6%). The main crystal phases of the fresh BOFS include brownmillerite ($Ca_2Fe_{1.014}Al_{0.986}O_5$), portlandite ($Ca(OH)_2$), wollastonite ($CaSiO_3$), β-larnite ($Ca_2SiO_4$), α-dicalcium silicate hydrate ($Ca_2(HSiO_4)(OH)$) and wustite (FeO). More details on the physico-chemical properties of BOFS can be found in our previous study [5].

In this study, three levels of carbonation degree of BOFS, i.e., low (~20%), medium (~50%), high (~90%), were selected for analytical tests. To generate the calibration (or standard) curve, the synthetic $CaCO_3$/BOFS mixtures were prepared by mixing different amounts of reference $CaCO_3$ powder (i.e., with a purity of 100%, purchased from J.T. Baker 1288-01 (NJ, USA)) with carbonated BOFS. Since the measured particle size of $CaCO_3$ after carbonation was 1–3 μm [2,5], the physico-chemical properties of the reaction product could be similar to the purchased reference $CaCO_3$.

2.2. Thermal analysis techniques

In TG analysis, the weight of sample at different temperatures was recorded under an assigned heating programs. By taking numerical derivation of the TG curve, a DTG plot can be obtained to provide the information on the temperature at the maximum peak and other important peak parameters. In a DSC, a sample cell and a

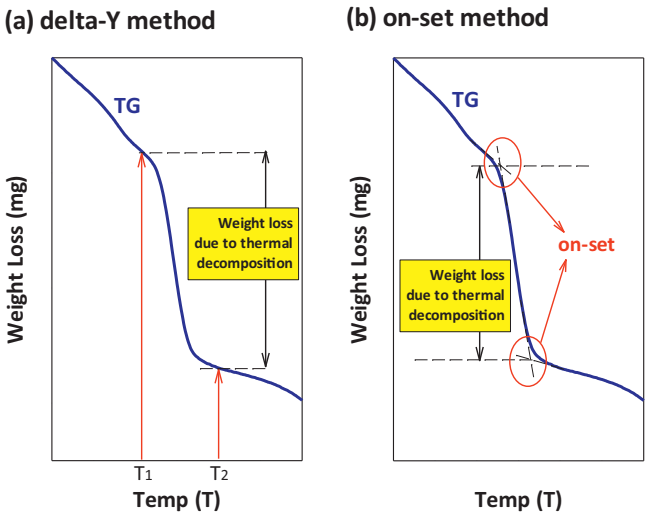

Fig. 1. Conventional methods on TG interpretation: (a) delta-Y and (b) on-set methods.

reference were heated equally according to a temperature regime, where the amount of energy absorbed or released by the sample can be measured with a DSC [27].

In this study, the $CaCO_3$ content in BOFS was examined by a TG analyzer (STA6000, PerkinElmer, USA) equipped with a DSC. The samples were heated directly from 50 to 950 °C at different heating rates (e.g., 5, 10, 15, 20, 25, 30 and 35 °C/min) under N_2 atmosphere at 20 mL/min. The accuracy of the furnace temperature was within ±0.5 °C 1–35 mg of reference $CaCO_3$ standards, carbonated BOFS samples, and synthetic $CaCO_3$/BOFS mixtures were placed in the platinum crucible in the TG analyzer. The wide variance of sample loading weight in TG analysis is intended to evaluate the precision and limitation of the proposed TG-DTG method. Moreover, blank correction runs were carried out to minimize the buoyancy effect. Furthermore, the evolved gas from the decomposition of the sample was subsequently routed towards an MS (Clarus® SQ8, PerkinElmer, USA) and an FTIR (Frontier™, PerkinElmer, USA) in a dynamic N_2 atmosphere, for detection of gaseous compounds released during heating.

2.3. Modified TG-DTG Interpretation for determination of $CaCO_3$ content

Fig. 3 illustrates the modified method of TG-DTG interpretation for determining the $CaCO_3$ content in alkaline solid wastes. Both the initial (T_1) and final (T_2) temperatures of $CaCO_3$ decomposition are determined by the extrapolated on-set. The extrapolated on-set is the point of intersection of the tangent drawn at the point of greatest slope on the leading edge of the peak with the extrapolated base line. Then, the weight loss due to $CaCO_3$ decomposition can be determined by (1) extending two straight line portions of the baseline before T_1 and after T_2; (2) making a vertical line pass through the midpoint (T_m) between T_1 and T_2; and (3) determining their intersections to the baselines and vertical line. The weight loss between these two intersections was attributed from the $CaCO_3$ decomposition within the solid samples.

Similarly, the DTG curve can be characterized by the temperature of extrapolated on-set drawn by the beginning (T_i) and final (T_f) of the peak. The center of temperature peak (T_p), half width ($W_{1/2}$),

Table 1
Ranges of decomposition temperature for $Ca(OH)_2$, $MgCO_3$ and $CaCO_3$ in different types of raw materials.

Type of materials[a]	Heating rate (°C/min)	Atmosphere	Sample weight (mg)	Decomposition temperature (°C)				Reference
				$Ca(OH)_2$	$MgCO_3$	$CaCO_3$	Carbonates	
Wollastonite	10	N_2	–	–	–	600–900	–	[11]
Serpentine	10	N_2	–	330–473	473–573	–	–	[12]
Serpentine	10	N_2			300–550			[13]
Concrete	10	–	225	430–530	–	780–900	650–950	[9]
Concrete	20	–	–	425–550	–	550–950	–	[14]
Mortar	10	Air	200	430–520		~750	–	[15]
Mortar/GBFS	10	N_2	–	>380	–	650–790	–	[16]
Steel slag	40	O_2	10–20	–	105–500	–	500–1000	[17]
Steel slag	15	N_2	~100	340–430	–	600–800	–	[3]
BOFS	10	N_2	10–20	–	–	500–780	–	[2]
BOFS	–	–	–	–	–	600–780	–	[18]
EAFS	–	Ar	–	~600	–	> 600	–	[19]
CKD/sludge	–	–	–	450–550	–	700–850	–	[20]
CKD	20	N_2	~22	300–500	–	500–800	–	[21]
MSWI-BA	10	Ar	20	–	–	600–750	–	[22]
MSWI-FA	10	–	–	–	–	–	450–900	[23]
APC residue	15	Air	500	400–500	–	750–850	600–850	[24]
APC residue	10	Air	–	400–450	–	650–800	–	[25]
Cockle shell	20	N_2	10–20	–	–	700–900	–	[26]
Synthesis carbonates	50	N_2	5–10	–	515–640	620–780	–	[7]

[a] GBFS: granulate blast furnace slag; BOFS: basic oxygen furnace slag; EAFS: electric arc furnace slag; CKD: cement kiln dust; MSWI: municipal solid waste incinerator; FA: fly ash; BA: bottom ash; APC: air pollution control.

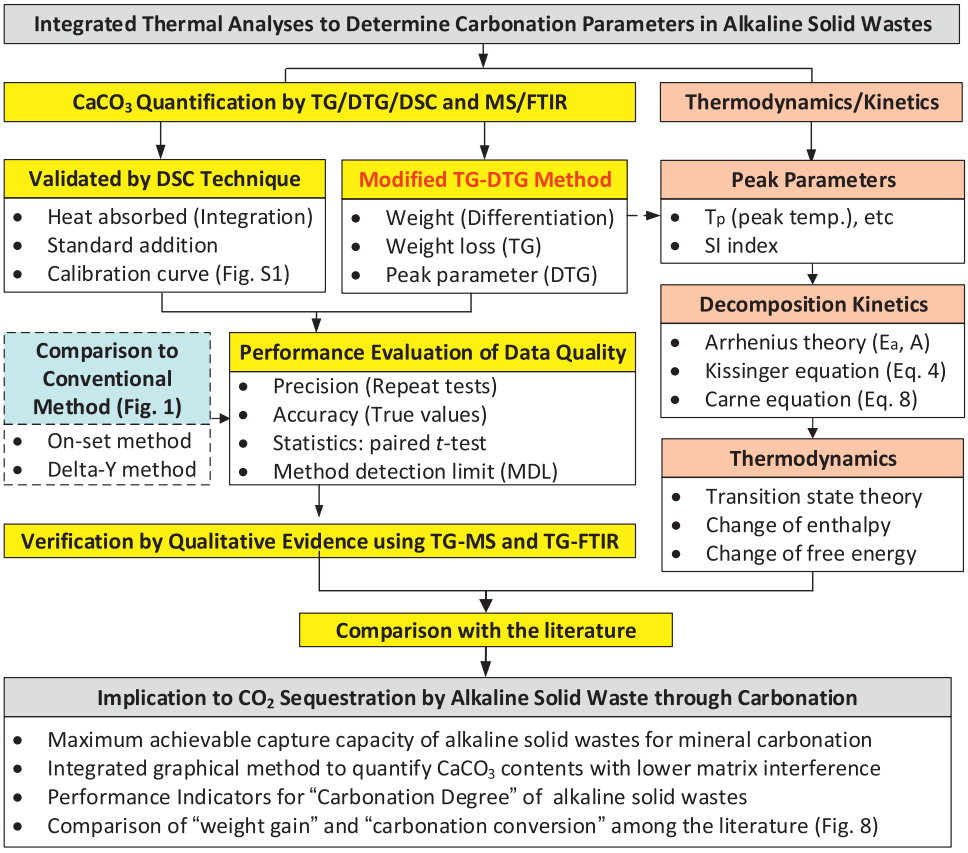

Fig. 2. Systematic approach to determination of carbonation parameters in alkaline solid wastes via integrated thermal analysis.

and peak width (W) can be also determined. The shape index (SI) of the DTG peak, defined as the absolute ratio of the slope of the tangents to the DTG peak at the inflection points, can be graphically determined as shown in Fig. 3.

2.4. Carbonation parameters of alkaline solid wastes

According to the modified TG-DTG method as shown in Fig. 3, the CO_2 content (denoted as "CO_2") in the original sample can be calculated by Eq. (1):

$$CO_2\,(\text{wt\%}) = \frac{\Delta m_{CO_2}}{m_{105^\circ C}} \times 100 \quad (1)$$

where Δm_{CO2} is the weight loss due to the $CaCO_3$ decomposition and m_{105} °C is the dry weight of the sample. Similarly, the % weight gain of the dry solid waste can be calculated using the value of CO_2 content, according to Eq. (2):

$$\text{Weight gain}\,(\%) = \frac{CO_2\,(\text{wt\%})}{100 - CO_2\,(\text{wt\%})} \times 100 \quad (2)$$

On the other hand, the carbonation conversion of solid waste (δ_{CaO}) can be determined by Eq. (3), assuming the calcium-bearing compositions are the main reaction species:

$$\delta_{CaO} = \frac{\frac{CO_2(\%)}{100-CO_2(\%)} \times \frac{1}{MW_{CO_2}}}{Ca_{total}/MW_{Ca}} = \frac{\frac{CO_2(\%)}{100-CO_2(\%)} \times \frac{1}{MW_{CO_2}}}{CaO_{total}/MW_{CaO}} \quad (3)$$

where MW_{CO2} is the molecular weight of CO_2 (i.e., 44 g/mol); MW_{Ca} and MW_{CaO} are the molecular weight of Ca (i.e., 40 g/mol) and CaO (i.e., 56 g/mol), respectively. Ca_{total} and CaO_{total} are the percent weight fraction of Ca (normally determined by XRF [6,7] or by ICP after total digestion [17]) and CaO (normally determined by XRF [28,29]) in the fresh solid sample, respectively.

2.5. Thermal decomposition kinetics and thermodynamics

The kinetic and thermodynamic parameters for the thermal decomposition of $CaCO_3$ in BOFS were determined, including apparent activation energy, kinetic exponent and pre-exponential factor in the Arrhenius equation, as well as the changes of entropy, enthalpy, and Gibbs free energy for the formation of the activated complex.

The Kissinger method has been extensively applied to determine the kinetics of thermal decomposition of a solid material using DTA, DTG or DSC, and the relevant activation energy and reaction order [30–34]. The generalized form of Kissinger equation for a non-isothermal kinetics can be expressed as Eq. (4), where the detailed derivations were presented in Appendix A:

$$\ln\left(\frac{\beta}{T_p^2}\right) = -\frac{E_a}{R}\frac{1}{T_P} + \ln\left(-\frac{ARf'(\alpha)}{E_a}\right) \quad (4)$$

where α is the reacted fraction, β is the heating rate (K/min), $f'(\alpha)$ is an algebraic function depending on the reaction mechanism, A is the pre-exponential factor (1/min), E_a is the apparent activation energy (kJ/mol), T_p is the absolute temperature of peak (K), and R is the universal gas constant (i.e., 8.314 J/K mol). The $f(\alpha)$ describing heterogeneous processes was controlled by the surface-reaction, and frequently expressed by the reaction order kinetic model [31], as shown in Eq. (5):

$$\frac{d\alpha}{dT} = \frac{A(1-\alpha)^n}{\beta}\exp\left(-\frac{E_a}{RT_p}\right) \quad (5)$$

where n is the kinetic exponent of thermal decomposition reaction, which can be directly determined by Eq. (6); or estimated from the

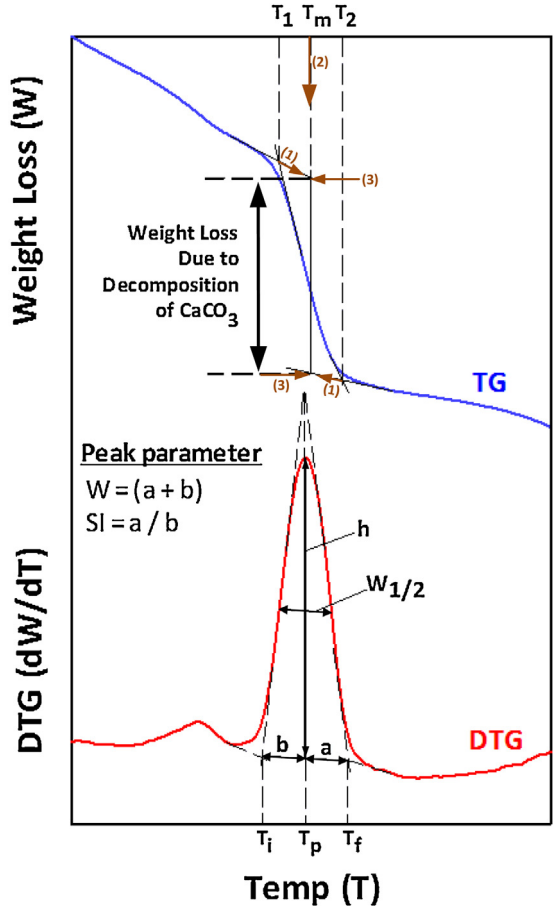

Fig. 3. Modified TG-DTG interpretation to determine $CaCO_3$ content in BOFS by both TG (upper curve) and peak parameters from DTG (lower curve).

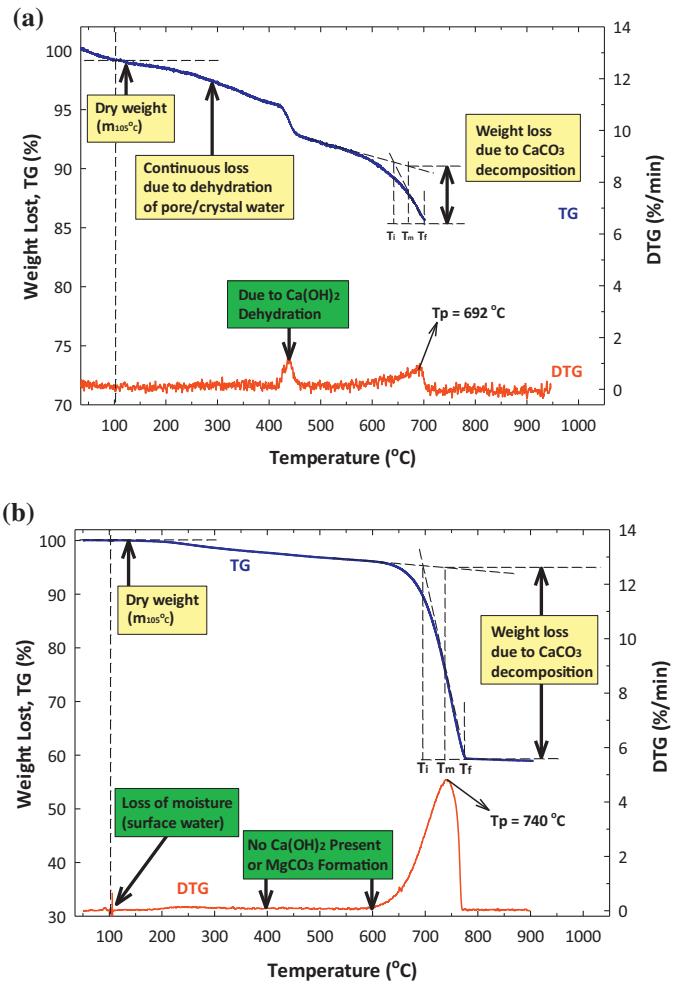

Fig. 4. TG-DTG plots for (a) fresh and (b) carbonated BOFS using the modified TG-DTG Interpretation method.

SI value using Eq. (7) [35]; or calculated from an empirical model proposed by Carne et al [36]. (Eq. (8)):

$$n = \frac{(1-\alpha_{max})}{d\alpha_{max}/dT}\frac{Af'(\alpha)}{\beta}\exp\left(-\frac{E_a}{RT_p}\right) \quad (6)$$

$$n = 1.26SI^{1/2} \quad (7)$$

$$\frac{1}{n} = -\frac{dln\beta}{d\left(1/T_p\right)}\frac{R}{E_a} \quad (8)$$

For thermodynamics of $CaCO_3$ decomposition in BOFS, the transition state theory (i.e., activated complex theory) was applied, which can be described by the general form of the Eyring equation as follows [30]:

$$A = \frac{e\chi k_B T_p}{h}\exp\left(\frac{\Delta S}{R}\right) \quad (9)$$

where e is the Neper number (i.e., 2.7183), χ is the transition factor (i.e., 1 for monomolecular reactions), k_B is the Boltzmann constant (i.e., 1.381×10^{-23} J K^{-1}), h is the Plank constant (i.e., 6.626×10^{-34} J s). Accordingly, the term of ΔS can be calculated based on the peak temperature (T_p) which characterizes the highest rate for $CaCO_3$ thermal decomposition in DTG plot.

The changes of the enthalpy (ΔH) and Gibbs free energy (ΔG) for the activated complex formation can be determined using the well-known thermo-dynamical Eqs. (10) and (11), respectively:

$$\Delta H = E_a - RT_p \quad (10)$$

$$\Delta G = \Delta H^{\neq} - T_p\Delta S \quad (11)$$

3. Results and discussion

3.1. Performance evaluation of modified TG-DTG interpretation

In this study, a modified TG-DTG interpretation was applied to determine the actual weight loss of the $CaCO_3$ decomposition in BOFS. Fig. 4 (a) and (b) show the TG-DTG plots of the fresh and carbonated BOFS, respectively. A continuous weight loss was observed at temperatures between 200 °C and 900 °C in both the fresh and carbonated BOFS. As aforementioned, this is attributed to the decomposition of various hydrates in BOFS, such as α-dicalcium silicate hydrate, which should be considered when evaluating the carbonate contents in alkaline solid wastes. Other major minerals in BOFS, such as brownmillerite, wollastonite and larnite, are relatively stable under the temperature range of TG analysis.

Except for the complex and hydrated compounds, the weight loss versus temperature for a material can be generally separated into (1) expulsion of surface water at 50–105 °C; (2) removal of pore water at 200 – 300 °C; (3) dehydration of crystal water (e.g., $Ca(OH)_2$) at 400–500 °C; (4) $MgCO_3$ decomposition at 500–630 °C; and (5) $CaCO_3$ decomposition at 600–850 °C. In the fresh BOFS, the thermal decomposition of portlandite ($Ca(OH)_2$) occurs at temperature 400–500 °C. After carbonation, however, there was lack of the peak for $Ca(OH)_2$ decomposition in BOFS, revealing that the $Ca(OH)_2$ was reacted with CO_2 during carbonation. Instead, a great weight loss at 600–800 °C was found in the carbonated BOFS, indicating the formation of $CaCO_3$ precipitates after carbonation.

There was no observation of $MgCO_3$ crystals in both fresh and carbonated BOFS due to no peak at 500–630 °C in DTG, which was in a good agreement with the XRD results in previous study [5,37]. The typical operating conditions for the formation of $MgCO_3$ precipitates via aqueous carbonation were found to be a temperature over 144 °C [38] and a reaction time of hours [39]. Instead, under the mild condition, metastable (amorphous) hydrated magnesium carbonate phases might be formed, if the ratio of Mg^{2+} to Ca^{2+} concentrations is higher than 0.5 [7]. However, it was noted that the leaching concentrations of magnesium ions from BOFS was much lower (e.g., 1.7 – 3.0 mg/L) than that of calcium ions (e.g., 876–2690 mg/L) [40]. Therefore, the formation of $MgCO_3$ crystal might be negligible due to its relatively lower contents in BOFS under improbable formation conditions. In other words, it was confirmed that the calcium-containing compositions in BOFS were the major species reacting with CO_2 to form $CaCO_3$ precipitate under the carbonation conditions performed in this study.

3.2. Validation of TG-DTG data quality by DSC technique: precision and accuracy

The data quality of the modified TG-DTG method, in terms of precision and accuracy, was validated by a DSC technique. The precision of the modified method was first evaluated and compared with conventional methods, i.e., the on-set and delta-Y methods, as shown in Table 2. In the case of the delta-Y method, the carbonate content was calculated directly from the weight loss that occurred between 500 °C and 900 °C. The results indicate that the precision of both the proposed method and the on-set method were quite high, with a relative standard deviation of less than 1% under different heating rates. However, the delta-Y method would be imprecise under high heating rate (e.g., 25 K/min), indicating that a reproducibility error might occur.

To evaluate the accuracy of the integrated thermal analyses, the DSC technique was coupled with the TG analysis to quantify the $CaCO_3$ content in BOFS. The DSC technique provides quantitative measurement on the heat released or absorbed by the specimen during the heating step. Theoretically, the pure $CaCO_3$ particles will start to decompose into CaO solid and CO_2 gas at temperatures above 600 °C. According to Eq. (12), the reaction heat for decomposing one mole of $CaCO_3$ particles at 1000 K is approximately 170.4 kJ [41].

$$CaCO_{3(s)} \xrightarrow[\Delta]{} CaO_{(s)} + CO_{2(g)}, \quad \Delta H^{o}_{1,000K} = 170.4\,kJ/mol \qquad (12)$$

Fig. S1 (see Appendix A) shows the TG-DTG and DSC profiles of reference pure $CaCO_3$ powder at temperatures ranging from 50 °C to 950 °C. It was observed that, between 580 °C and 820 °C, the TG curve shows a weight loss of about 44%, attributed to the thermal decomposition of $CaCO_3$. The peak of the DTG curve was found to be around 766 °C, accomplished by an endothermic phenomenon of a total of 1.78 kJ/g from the DSC result. Since the amounts of heat absorbed can be converted into the weight of $CaCO_3$ decomposed according to Eq. (12), the correlation between DSC and TG measurements can be established. With the above findings, the correlation between the amounts of $CaCO_3$ decomposition (i.e., integrated thermal analyses) and heat absorbed (i.e., DSC result) was established as shown in Fig. 5. The results indicate that the values of relative percent difference between the weights of $CaCO_3$ determined by thermography and those calculated from DSC are 1.34 ± 0.20%.

Table 2 summarizes the accuracy of the modified TG-DTG interpretation and the conventional methods, i.e., the on-set and delta-Y methods, by coupling the DSC measurement as the true value of $CaCO_3$ content. The results indicate that the modified TG-DTG method exhibits the highest accuracy, with a relative percent difference of less than 2.5%, among the three methods, i.e., the modified TG-DTG interpretation, conventional on-set and delta-Y methods. Compared to the others, the effect of heating rate on measurement obtained from the proposed method was not significant. However, the delta-Y method resulted in the greatest deviation, especially at a higher heating rate (i.e., up to 16% at 25 °C/min).

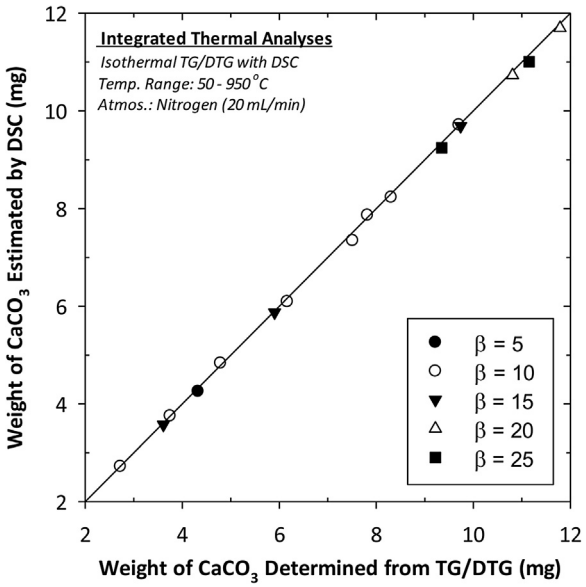

Fig. 5. Correlation of TG-DTG and DSC results for reference pure $CaCO_3$ powder under thermal decomposition.

The actual amounts of $CaCO_3$ in a solid sample can be generally defined as "purity," i.e., gram of $CaCO_3$ per gram of solid sample, which should be proportional to the amounts of CO_2 released during the thermal decomposition. According to the stoichiometric relationship shown in Eq. (12), one gram of $CaCO_3$ will result in 0.44 g of CO_2 released during thermal analysis. Therefore, from the theoretical consideration approach, the plot of CO_2 (wt%) versus purity should be a straight line with a slope of 0.44 and an intercept of zero. Fig. S2 (see Appendix A) shows the regression results by applying the integrated thermal analyses, which also could provide evidence of the high accuracy of the analysis results. In other words, the results obtained by the modified TG-DTG interpretation can be validated by both the DSC technique and theoretical consideration, indicating the accuracy of the modified method in the case of synthetic BOFS/$CaCO_3$ mixtures.

Since the analytical data from TG-DTG and DSC curves shows a normal distribution, they can be examined by paired samples *t*-tests to determine whether two sets of data are significantly different from each other. Table S1 (see Appendix A) presents the results of paired samples *t*-tests, which indicate that the calculated *t*-value of 1.595 was less than the tabulated *t*-value of 2.201, thereby accepting the null hypothesis. No difference was thus found in $CaCO_3$ contents calculated from the integrated thermal analyses on the modified TG-DTG interpretation and DSC analysis ($p = 0.139$), with a Pearson's correlation coefficient of 0.9997. This suggests that the modified TG-DTG interpretation was applicable to provide a precise and accurate analysis of $CaCO_3$ contents in BOFS.

3.3. Verification by TG-FTIR and TG-MS: qualitative observations

As the aforementioned challenges, the weight loss between 500 °C and 900 °C would be simultaneously attributed to the decomposition of carbonates (release CO_2) and hydrates (release H_2O). Therefore, weight loss during thermal degradation was correlated with the evolved gas analysis by TG-FTIR and TG-MS to

Table 2
Precision and Accuracy of modified TG-DTG method comparable with conventional methods for different levels of sample weights.[a]

	Modified TG-DTG method (this study)				On-set method (conventional)				Delta-Y method (conventional)			
β (K/min)	Mean[b](%)	StDev. [c](%)	RSD[d](%)	RPD[e] (%)	Mean(%)	St Dev.(%)	RSD(%)	RPD[e] (%)	Mean(%)	StDev. (%)	RSD(%)	RPD[e] (%)
5	99.39	0.25	0.25	1.32 ± 0.49	98.69	0.39	0.40	1.08 ± 1.27	98.92	0.79	0.80	1.16 ± 0.83
10	98.58	0.70	0.71	1.37 ± 0.88	98.64	0.70	0.71	1.43 ± 0.87	98.99	0.31	0.31	1.01 ± 0.39
15	98.82	0.32	0.33	1.25 ± 0.40	98.76	0.32	0.32	1.19 ± 0.41	99.05	0.32	0.32	0.96 ± 0.40
20	98.92	0.41	0.42	1.51 ± 0.29	98.54	0.24	0.25	1.82 ± 2.10	98.84	0.42	0.42	2.25 ± 3.05
25	98.93	0.29	0.30	1.23 ± 0.49	98.77	0.39	0.40	1.08 ± 0.37	96.03	7.04	7.33	4.27 ± 9.57
Precision	Superior (%RSD = 0.40 ± 0.25)				Superior (%RSD = 0.42 ± 0.24)				Fair (%RSD = 1.84 ± 4.27)			
Accuracy	Superior (%RPD = 1.34 ± 0.20)				Good (%RPD = 1.42 ± 0.45)				Fair (%RPD = 1.93 ± 1.74)			

[a] Weights of sample were categorized into five levels: lowest (1–5 mg), low (5–10 mg), medium (10–15 mg), high (15–25 mg), and highest (25–35 mg).
[b] Mean: average value in measured $CaCO_3$ purity among five repeated analyses ($N = 5$).
[c] StDev. : standard deviation among five analyses.
[d] RSD: relative standard deviation (S.D. between average purity value/average of purity) × 100.
[e] RPD: Relative percent difference for accuracy evaluation, with 95% confidence interval.

identify the types of volatiles and/or gases released. Figs. S3(a) and S3(b) (see Appendix A) show the FTIR spectra of the fresh and carbonated BOFS, respectively. Based on the FTIR results of the fresh BOFS, the first peaks occurred continuously at 100–200 °C and 400–500 °C due to the removal of absorbed surface water ($\delta_{(O-H)}$ bending mode at 1508 cm^{-1}) and crystal water ($\delta_{(O-H)}$ bending mode at 1578 cm^{-1}), respectively. The second more intense peak was observed at 700–800 °C, mainly associated with the CO_2 signals (i.e., asymmetric C—O stretching vibration at 1454 cm^{-1}). In the case of carbonated BOFS, however, the main FTIR peaks of evolution took place in the temperature range of 700–800 °C, indicating a great amount of CO_2 released (characteristic bands at 2,363/1,454/688 cm^{-1}).

TGA coupled with MS was carried out on both fresh and carbonated BOFS, as shown in Figs. Fig. 6 (a) and (b), respectively. The dissociation of the phases containing H_2O in fresh BOFS comprises three peaks, which occur at 102 °C, 375 °C and 443 °C. These can result from evaporation of surface water, evaporation of pore water, and dehydration of crystal water (i.e., $Ca(OH)_2$), respectively. On the other hand, in the case of carbonated BOFS, the results show that two peaks for H_2O signal were observed at 106 °C and 238 °C, indicating subsequent removal of surface water and pore water. The $Ca(OH)_2$ content should be eliminated after carbonation because no H_2O signal was observed at 400–500 °C. In addition, the dehydration of different hydrates was found to occur continuously between 50 and 800 °C and was especially pronounced before 700 °C, due to the series of H_2O signal in the evolved gas analysis results, which provides the evidence to the observations in TG-DTG plot.

In the TG-MS pattern, CO_2 evolved gas was observed at 695 °C in fresh BOFS, which came from the decomposition of $CaCO_3$. Similar results were observed in the carbonated BOFS that the loss of mass occurring between 650 and 750 °C corresponds mainly to CO_2 emissions. It can be deduced that they correspond to the decomposition of $CaCO_3$ with a high temperature peak of 736 °C, which confirmed that the carbonate product is a crystallized $CaCO_3$. Furthermore, no peak of CO_2 signal was observed at 500–600 °C after carbonation, indicating the decomposition of $MgCO_3$ crystal was not detected, which provided the rationale that the formation of $MgCO_3$ precipitates was negligible in this study.

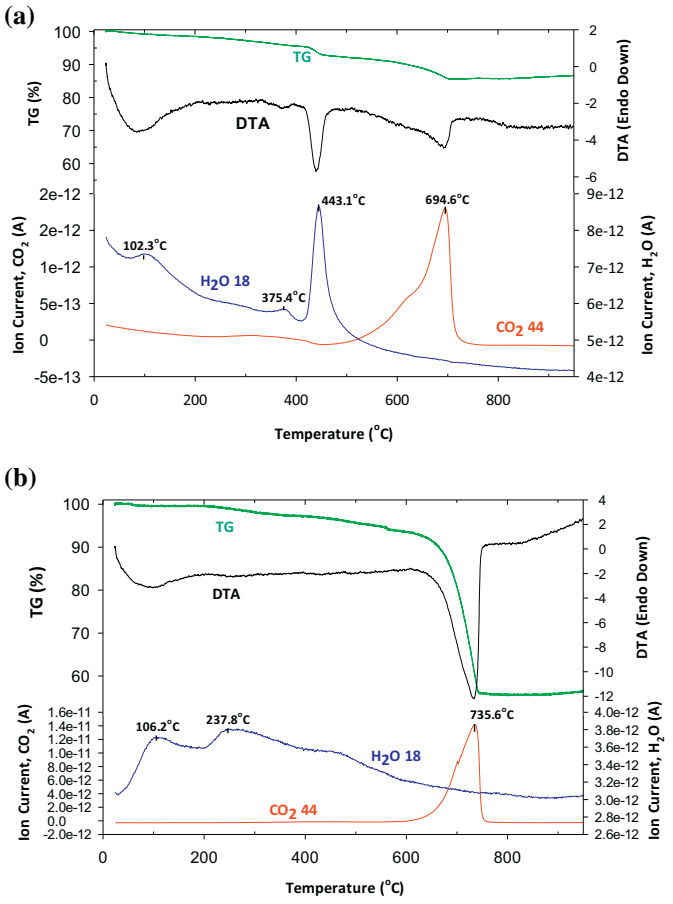

Fig. 6. Plots of mass change (TG Analysis) and of mass spectroscopy (ion current for H_2O mass number 18 and CO_2 mass number 44) in (a) fresh and (b) carbonated BOFS.

3.4. Principles of thermal decomposition for $CaCO_3$ in BOFS: kinetics and thermodynamics

The kinetic parameters including E_a, n and A values for the thermal decomposition of $CaCO_3$ in BOFS were calculated. Table S2 (see Appendix A) presents the influence of heating rate on important peak parameters, such as T_i, T_e, W, $W_{1/2}$, H and SI value. The results indicate that the peak temperature (T_p) of $CaCO_3$ decomposition increases with the increase of the heating rate. As shown in Fig. 7, the value of E_a estimated from the slope of the Kissinger plot (Eq. (4)) yields 197.7 ± 5.5 kJ/mol, with an R^2 value of 0.995. It was noted that the activation energy increases as the particle size increases [26,42]. The E_a values experimentally determined in the literature were found to be in the ranges of 139.0–190.4 and 119.7–179.4 kJ/mol for the cases of pure $CaCO_3$ powder [8,32,33,42] and $CaCO_3$ mixture [26,30,43], respectively. In this study, the obtained E_a value (i.e., 198 kJ/mol) was higher than the value of theoretical activation energy for thermal decomposition of isolated calcite $CaCO_3$ (i.e., 175 kJ/mol) [43]. This may be because calcite was formed inside BOFS particles and/or on the surface of BOFS parti-

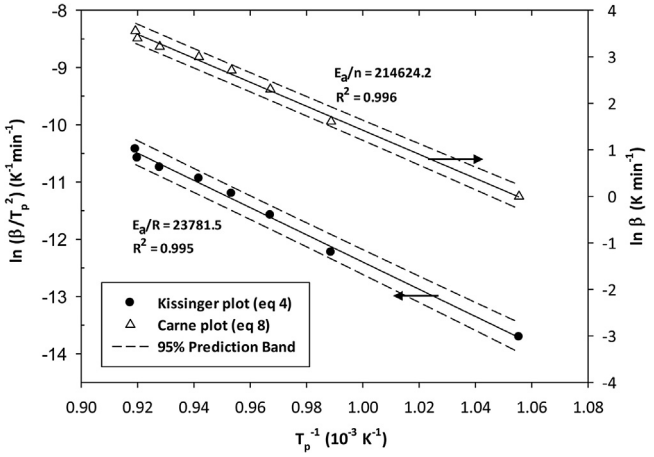

Fig. 7. Kissinger plot and Carne plot used for evaluation of apparent activation energy and reaction order of $CaCO_3$ thermal decomposition in BOFS.

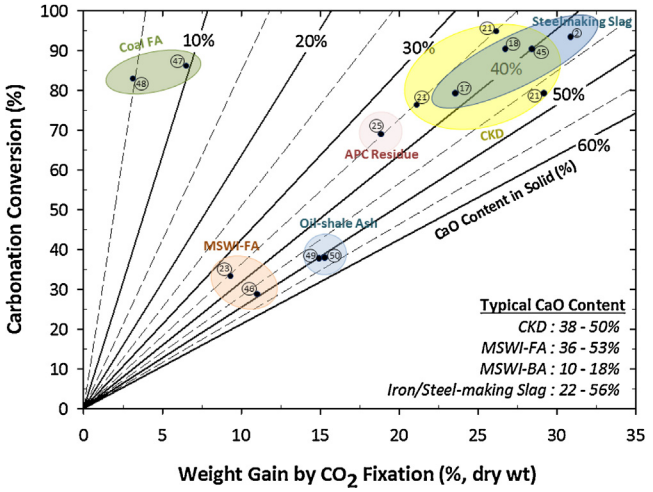

Fig. 8. Relationship between carbonation conversion of solid waste and weight gain per dry weight. CKD: cement kiln dust; MSWI: municipal solid waste incinerator; FA: fly ash; APC: air pollution control. The numerical values shown in the circle denote the Reference number.

cles, thereby requiring extra energy to overcome the barrier of an impure layer.

The n value was calculated using several proposed techniques including the reaction order model (Eq. (6)), the *SI* of peak (Eq. (7)) and the Carne equation (Eq. (8)), as presented in Table 3. The n values obtained from the reaction order model and the SI of peak were from 0.11 to 2.58 and 0.47 to 0.81, respectively, which indicate that the n value is sensitive to heating conditions. The methods applied for calculation of the n value provide considerably different results. On the other hand, based on the Carne plot, the n value was estimated to be 0.92 ± 0.03, with the highest R^2 value of 0.996 among all the applied methods. Therefore, the $CaCO_3$ decomposition in BOFS was considered as a first order reaction, implying interface-controlled growth with grain boundary nucleation after saturation [44]. The results (i.e., $n \cong 1$) were also consistent with the findings presented in the literature [26,30,32,33,42,43]. As a result, the n value from the Carne method was utilized to calculate the pre-exponential factor (A). Substitution of E_a and n values into Eq. (5) provides an average value of A of $(2.20 \pm 0.01) \times 10^9$ min^{-1}, where the A value regularly increased with the heating rate.

Accordingly, the thermodynamic parameters including ΔS, ΔH, and ΔG was determined using general equations as shown in the Appendix A. As shown in Table 3, the average value of ΔS was estimated to be −118.82 J/mol K, which indicated that the formation of the activated complex exhibited a more organized structure than the initial substance. In addition, the average values of ΔH and ΔG were estimated to be 189.04 kJ/mol and 313.16 kJ/mol, respectively. Table 4 summarizes the comparison of the kinetics and thermodynamics data for decomposition of $CaCO_3$ precipitates via different analytical methods in the literature. In this study, the ΔH values for $CaCO_3$ decomposition are close to the E_a values; however, significant differences between the values of ΔH and ΔS are observed, which is similar to the findings reported in the literature [44]. The ΔS, ΔH, and ΔG values experimentally determined by Georgieva et al [30]. were found to be in the ranges of 148.7–181.5 J/mol·K, 125.3–158.7 kJ/mol, and 297.9–304.9 kJ/mol, respectively, which was in a good agreement with those in this study.

3.5. Implication to CO_2 sequestration by alkaline wastes

Alkaline solid wastes, such as steelmaking slag and fly ash, have been recognized as effective materials for CO_2 sequestration by mineral carbonation. In most of the studies reported in the literature, both the weight gain (Eq. (2)) and/or carbonation conversion (Eq. (3)) determined by TGA were frequently expressed as the degree of carbonation for one target material. Fig. 8 shows the relationship between carbonation conversion and weight gain of alkaline solids, which can conveniently identify the performances of mineral carbonation for CO_2 sequestration as suggested in the literature [2,17,18,21,23,25,45–50]. The plot of carbonation conversion versus weight gain is a straight line, and the slope of the straight line is related to the CaO content in the solid. For instance, the steelmaking slag and cement kiln dust exhibit the relatively higher CaO content and CO_2 capture capacity via the maximum achievable conversion technologies as reported in the literature [12,17,18,45]. Although a higher carbonation conversion of coal fly ash can be achieved, the CaO content of coal fly ash is low (i.e., 5–10%), thereby resulting in a relatively low CO_2 capture capacity.

Rapid, accurate and precise determination of the contents of $CaCO_3$ formation in the course of mineral carbonation is crucial for assessing the potential for CO_2 capture by alkaline wastes, as well as providing scientific data for interpretation of the carbonation reaction kinetics. In this study, the proposed integrated thermal analysis should be generally applicable to various alkaline solid wastes from different types of carbonation process. The standard operation procedure of thermal analysis is highlighted as follows:

(1) Dry samples at 105 °C for at least 30 min to remove the adsorbed water before analysis.
(2) Locate 3–10 mg of solid samples in a platinum crucible, and put in TG analyzer.
(3) Heat sample directly from 50 to 950 °C at 10–20 °C/min under N_2 atmosphere.
(4) Apply the modified TG-DTG interpretation (Fig. 3) to determine the weight loss of certain compound.
(5) Combine with other qualitative analyses (such as MS) to confirm the species of evolved gas within the temperature ranges of decomposition.

By the modified TG-DTG interpretation, there is a positive correlation between $CaCO_3$ content in alkaline wastes and its reactivity with CO_2 through mineral carbonation. The matrix interference due to Ca-Al-Si hydrate compounds presented in alkaline wastes can be reduced to a level of 10^{-3}. In accordance with NIEA-PA107, the method detection limit of the proposed method was found to be 0.70%, with a relatively higher precision (0.40 ± 0.25%) and accuracy (1.34 ± 0.20%).

Table 3
Values of kinetic parameters and the corresponding thermodynamic parameters determined by Kissinger calculation procedure.

β (K/min)	$\times 10^{-3}$ $1/T_p$ (1/K)	$(1-\alpha_{max})$[a]	$\times 10^{-2}$ $d\alpha_{max}/dT$ (1/K)[a]	n			$\times 10^9$ A	ΔS	ΔH	ΔG
				Kissinger (Eq. (6))	Kissinger (Eq. (7))	Carne (Eq. (8))	(1/min)[b]	(J/mol K)	(kJ/mol)	(kJ/mol)
1	1.056	0.646 ± 0.008	0.657 ± 0.005	2.58	0.47	0.92	2.194	−118.05	189.84	301.69
5	0.989	0.676 ± 0.018	2.542 ± 0.065	0.68	0.55	0.92	2.202	−118.57	189.31	309.23
10	0.967	0.671 ± 0.007	4.572 ± 0.115	0.31	0.64	0.92	2.201	−118.75	189.12	311.91
15	0.953	0.694 ± 0.002	6.507 ± 0.250	0.21	0.65	0.92	2.207	−118.85	189.00	313.66
20	0.942	0.693 ± 0.004	8.401 ± 0.069	0.16	0.69	0.92	2.207	−118.95	188.89	315.20
25	0.928	0.694 ± 0.005	9.081 ± 0.131	0.17	0.73	0.92	2.207	−119.08	188.76	317.09
30	0.920	0.701 ± 0.005	10.35 ± 0.380	0.15	0.79	0.92	2.209	−119.14	188.68	318.19
35	0.919	0.702 ± 0.007	12.28 ± 0.340	0.11	0.81	0.92	2.209	−119.15	188.67	318.29

[a] Data with 95% confidence interval.
[b] The pre-exponential factor was determined by Eq. (4) and Eq. (8) (n = 0.92).

Table 4
Comparison of thermal decomposition kinetics of $CaCO_3$ precipitates in this study and those in the literature.

Exp.	Method	E_a (kJ mol^{-1})	Ln (A) (min^{-1})	n	$-\Delta S$ (J mol^{-1} K^{-1})	ΔH (kJ mol^{-1})	ΔG (kJ mol^{-1})	Types of $CaCO_3$	Particle size (μm)	$f(\alpha)$[a]	Reference
TG	Non-isothermal (N_2)	150	–	1	–	–	–	Pure calcite	50–100	F_1,	[28]
		163	–	1	–	–	–		100–160	KM	
TG	Isothermal (N_2)	162.5	–	1.11	–	–		Pure calcite	–	R_2, KM	[18]
TG	Isothermal	139.0	22.5	1	–	–	–	Pure calcite	~225	GPM	[8]
TG	Non-isothermal (air)	180.2	17.69	1	–	129.6	–	Pure calcite	~100	F_1, CRM	[17]
TG	Non-isothermal (N_2)	159.3	17.82	0.67	149.1	151.3	297.9	Pure calcite	–	R_3, KM	[15]
TG	Non-isothermal (N_2)	179.4	–	1	–	–	–	Formed in cockle shell	125–250	F_1, SCM	[27]
TG	Isothermal (Air)	119.7	–	–	–	–	–	Formed in white-body wall tile	~350	SCM	[29]
DTG	Non-isothermal (N_2)	197.7	21.51	0.92	118.8	189.0	313.2	Formed in steelmaking slag	~82	F_1	This study

[a] KM: Kissinger method; GPM: grainy pellet model (assuming both the chemical reaction on microcrystal and CO_2 diffusion through particle are rate-limiting steps); SCM: shrinking core model; CRM: Coats-Redfern method.

4. Conclusions

A modified TG-DTG interpretation was developed in this study and validated with DSC analysis. The proposed method exhibits a relatively higher precision and accuracy than conventional methods. In addition, the kinetic and thermodynamic parameters of $CaCO_3$ thermal decomposition in solid waste were determined. The apparent activation energy and frequency factor corresponds to 197.7 ± 5.5 kJ mol^{-1} and $(2.20 \pm 0.01) \times 10^9$ min^{-1}, respectively. From the slope of the Carne plot, the apparent kinetic exponent (n) was estimated at 0.92 ± 0.03, which indicates the interface controlled growth with grain boundary nucleation after saturation. The thermodynamic parameters including $\Delta S^{\ddagger}$, $\Delta H^{\ddagger}$ and $\Delta G^{\ddagger}$ were estimated to be -118.82 J mol^{-1} K^{-1}, 189.04 kJ mol^{-1} and 313.16 kJ mol^{-1}, respectively. Furthermore, this article provides the technical guideline and criteria on evaluating the CO_2 fixation performance of industrial solid wastes via accelerated carbonation. The different types of performance indicators, i.e., weight gain and carbonation conversion, for CO_2 fixation using carbonation were comprehensively reviewed and compared to the results obtained in this investigation.

Acknowledgements

The authors wish to thank the Ministry of Science and Technology (MOST) of Taiwan (R.O.C.) for the financial support under grant number MOST 105-3113-E-007-001. In addition, Prof. H. Kim was supported by the R&D Program of MKE/KEIT (10037331, Development of Core Water Treatment Technologies based on Intelligent BT-NT-IT Fusion Platform).

Appendix A. Supplementary data

Supplementary data associated with this article can be found, in the online version, at http://dx.doi.org/10.1016/j.indcrop.2015.12.082.

References

[1] S.-Y. Pan, E.E. Chang, P.-C. Chiang, CO_2 capture by accelerated carbonation of alkaline wastes: a review on its principles and applications, Aerosol Air Qual. Res. 12 (2012) 770–791.
[2] E.E. Chang, S.Y. Pan, Y.H. Chen, C.S. Tan, P.C. Chiang, Accelerated carbonation of steelmaking slags in a high-gravity rotating packed bed, J. Hazard Mater. 227–228 (2012) 97–106.
[3] R.M. Santos, J. Van Bouwel, E. Vandevelde, G. Mertens, J. Elsen, T. Van Gerven, Accelerated mineral carbonation of stainless steel slags for CO_2 storage and waste valorization: effect of process parameters on geochemical properties, Int. J. Greenhouse Gas Control 17 (2013) 32–45.
[4] I.M. Power, A.L. Harrison, G.M. Dipple, S.A. Wilson, P.B. Kelemen, M. Hitch, G. Southam, Carbon mineralization: from natural analogues to engineered systems, Rev. Mineral. Geochem. 77 (2013) 305–360.
[5] S.Y. Pan, P.C. Chiang, Y.H. Chen, C.S. Tan, E.E. Chang, Ex Situ CO_2 capture by carbonation of steelmaking slag coupled with metalworking wastewater in a rotating packed bed, Environ. Sci. Technol. 47 (2013) 3308–3315.
[6] S. Tian, J. Jiang, Sequestration of flue gas CO_2 by direct gas-solid carbonation of air pollution control system residues, Environ. Sci. Technol. 46 (2012) 13545–13551.
[7] T. Hosseini, C. Selomulya, N. Haque, L. Zhang, Investigating the effect of the Mg^{2+}/Ca^{2+} molar ratio on the carbonate speciation during the mild mineral carbonation process at atmospheric pressure, Energy Fuel 29 (2015) 7483–7496.
[8] A. Escardino, J. García-Ten, C. Feliu, A. Saburit, V. Cantavella, Kinetic study of the thermal decomposition process of calcite particles in air and CO_2 atmosphere, J. Ind. Eng. Chem. 19 (2013) 886–897.
[9] G. Villain, M. Thiery, G. Platret, Measurement methods of carbonation profiles in concrete: thermogravimetry, chemical analysis and gammadensimetry, Cem. Concr. Res. 37 (2007) 1182–1192.
[10] B.K. Marsh, R.L. Day, Pozzolanic and cementious reactions of fly ash in blended cement pastes, Cem. Concr. Res. 18 (1988) 301–310.
[11] C.Y. Tai, W.R. Chen, S.-M. Shih, Factors affecting wollastonite carbonation under CO_2 supercritical conditions, AIChE J. 52 (2006) 292–299.
[12] W. Li, B. Li, Z. Bai, Electrolysis and heat pretreatment methods to promote CO_2 sequestration by mineral carbonation, Chem. Eng. Res. Des. 87 (2009) 210–215.
[13] S. Teir, S. Eloneva, C. Fogelholm, R. Zevenhoven, Fixation of carbon dioxide by producing hydromagnesite from serpentinite, Appl. Energy 86 (2009) 214–218.
[14] C. Chang, J. Chen, The experimental investigation of concrete carbonation depth, Cem. Concr. Res. 36 (2006) 1760–1767.
[15] M. Thiery, G. Villain, P. Dangla, G. Platret, Investigation of the carbonation front shape on cementitious materials: effects of the chemical kinetics, Cem. Concr. Res. 37 (2007) 1047–1058.

[16] S.A. Bernal, R.M. de Gutierrez, J.L. Provis, V. Rose, Effect of silicate modulus and metakaolin incorporation on the carbonation of alkali silicate-activated slags, Cem. Concr. Res. 40 (2010) 898–907.
[17] W.J.J. Huijgen, G.J. Witkamp, R.N.J. Comans, Mineral CO_2 sequestration by steel slag carbonation, Environ. Sci. Technol. 39 (2005) 9676–9682.
[18] Y.-T. Chen, Effects of Process Variables on the Conversion of BOF Slag to Carbonate, Graduate Institute of Chemical Engineering, National Taiwan University, Taipei, Taiwan, 2008, pp. 122.
[19] S.N. Lekakh, C.H. Rawlins, D.G.C. Robertson, V.L. Richards, K.D. Peaslee, Kinetics of aqueous leaching and carbonization of steelmaking slag, Metall. Mater. Trans. B 39 (2008) 125–134.
[20] Q. Chen, L. Zhang, Y. Ke, C. Hills, Y. Kang, Influence of carbonation on the acid neutralization capacity of cements and cement-solidified/stabilized electroplating sludge, Chemosphere 74 (2009) 758–764.
[21] D.N. Huntzinger, J.S. Gierke, S.K. Kawatra, T.C. Eisele, L.L. Sutter, Carbon dioxide sequestration in cement kiln dust through mineral carbonation, Environ. Sci. Technol. 43 (2009) 1986–1992.
[22] E. Rendek, G. Ducom, P. Germain, Carbon dioxide sequestration in municipal solid waste incinerator (MSWI) bottom ash, J. Hazard. Mater. 128 (2006) 73–79.
[23] X. Li, M.F. Bertos, C.D. Hills, P.J. Carey, S. Simon, Accelerated carbonation of municipal solid waste incineration fly ashes, Waste Manage. 27 (2007) 1200–1206.
[24] G. Cappai, S. Cara, A. Muntoni, M. Piredda, Application of accelerated carbonation on MSW combustion APC residues for metal immobilization and CO_2 sequestration, J. Hazard. Mater. 207–208 (2012) 159–164.
[25] R. Baciocchi, G. Costa, E. Di Bartolomeo, A. Polettini, R. Pomi, The effects of accelerated carbonation on CO_2 uptake and metal release from incineration APC residues, Waste Manage. 29 (2009) 2994–3003.
[26] M. Hohamed, S. Yusup, S. Maitra, Decomposition study of calcium carbonate in cockle shell, J. Eng. Sci. Technol. 7 (2012) 1–10.
[27] R.F. Speyer, Thermal Analysis of Materials, Marcel Dekker Inc., New York, 1994.
[28] M. Uibu, M. Uus, R. Kuusik, CO_2 mineral sequestration in oil-shale wastes from Estonian power production, J. Environ. Manage. 90 (2009) 1253–1260.
[29] N.L. Ukwattage, P.G. Ranjith, M. Yellishetty, H.H. Bui, T. Xu, A laboratory-scale study of the aqueous mineral carbonation of coal fly ash for CO_2 sequestration, J. Clean. Prod. 103 (2015) 665–674.
[30] V. Georgieva, L. Vlaev, K. Gyurova, Non-isothermal degradation kinetics of $CaCO_3$ from different origin, J. Chem. 2013 (2013) 1–12.
[31] P. Ptáček, F. Šoukal, T. Opravil, J. Havlica, J. Brandštetr, The kinetic analysis of the thermal decomposition of kaolinite by DTG technique, Powder Technol. 208 (2011) 20–25.
[32] X.-G. Li, Y. Lv, B.-G. Ma, W.-Q. Wang, S.-W. Jian, Decomposition kinetic characteristics of calcium carbonate containing organic acids by TGA, Arabian J. Chem. (2013).
[33] I. Halikia, L. Zoumpoulakis, E. Christodoulou, D. Prattis, Kinetic study of the thermal decomposition of calcium carbonate by isothermal methods of analysis, Eur. J. Miner. Process. Environ. Prot. 1 (2001) 89–102.
[34] D. Chen, X. Gao, D. Dollimore, A generalized form of the Kissinger equation, Thermochim. Acta 215 (1993) 109–117.
[35] H.E. Kissinger, Reaction kinetics in differential thermal analysis, Anal. Chem. 29 (1957) 1702–1706.
[36] L.W. Carne, P.J. Dynes, D.H. Kaelble, Analysis of curing kinetics in polymer composites, J. Polym. Sci. 11 (1973) 533–540.
[37] S.Y. Pan, Y.H. Chen, C.D. Chen, A.L. Shen, M. Lin, P.C. Chiang, High-gravity carbonation process for enhancing CO_2 fixation and utilization exemplified by the steelmaking industry, Environ. Sci. Technol. 49 (2015) 12380–12387.
[38] S. Teir, Fixation of Carbon Dioxide by Producing Carbonates from Minerals and Steelmaking Slags, Department of Energy Technology, Helsinki University of Technology, 2008.
[39] E.E. Chang, A.-C. Chiu, S.-Y. Pan, Y.-H. Chen, C.-S. Tan, P.-C. Chiang, Carbonation of basic oxygen furnace slag with metalworking wastewater in a slurry reactor, Int. J. Greenhouse Gas Control 12 (2013) 382–389.
[40] S.Y. Pan, P.C. Chiang, Y.H. Chen, C.D. Chen, H.Y. Lin, E.E. Chang, Systematic approach to determination of maximum achievable capture capacity via leaching and carbonation processes for alkaline steelmaking wastes in a rotating packed bed, Environ. Sci. Technol. 47 (2013) 13677–13685.
[41] S. Tian, J. Jiang, D. Hosseini, A.M. Kierzkowska, Q. Imtiaz, M. Broda, C.R. Mîller, Development of a steel-slag-based, iron-functionalized sorbent for an autothermal carbon dioxide capture process, ChemSusChem 8 (2015) 3839–3846.
[42] J.M. Criado, A. Ortega, A study of the influence of particle size on the thermal decomposition of $CaCO_3$ by means of constant rate thermal analysis, Thermochim. Acta 195 (1992) 163–167.
[43] A. Escardino, J. García-Ten, C. Feliu, A. Moreno, Calcium carbonate thermal decomposition in white-body wall tile during firing. I. Kinetic study, J. Eur. Ceram. Soc. 30 (2010) 1989–2001.
[44] J. Málek, The applicability of Johnson–Mehl–Avrami model in the thermal analysis of the crystallization kinetics of glasses, Thermochim. Acta 267 (1995) 61–73.
[45] S. Eloneva, S. Teir, J. Salminen, C.J. Fogelholm, R. Zevenhoven, Steel converter slag as a raw material for precipitation of pure calcium carbonate, Ind. Eng. Chem. Res. 47 (2008) 7104–7111.
[46] Q. Wang, P. Yan, Hydration properties of basic oxygen furnace steel slag, Constr. Build. Mater. 24 (2010) 1134–1140.
[47] C. Regina Costa, P. Olivi, Effect of chloride concentration on the electrochemical treatment of a synthetic tannery wastewater, Electrochim. Acta 54 (2009) 2046–2052.
[48] G. Montes-Hernandez, R. Perez-Lopez, F. Renard, J.M. Nieto, L. Charlet, Mineral sequestration of CO_2 by aqueous carbonation of coal combustion fly-ash, J. Hazard. Mater. 161 (2009) 1347–1354.
[49] M. Uibu, R. Kuusik, Mineral trapping of CO_2 via oil shale ash aqueous carbonation: controlling mechanism of process rate and development of continuous-flow reactor system, Oil Shale 26 (2009) 40.
[50] O. Velts, M. Uibu, J. Kallas, R. Kuusik, Waste oil shale ash as a novel source of calcium for precipitated calcium carbonate: carbonation mechanism, modeling, and product characterization, J. Hazard. Mater. 195 (2011) 139–146.